Vector Observation-Aided Attitude/Attitude-Rate Estimation Using Global Positioning System Signals

Yaakov Oshman* and F. Landis Markley†
NASA Goddard Space Flight Center, Greenbelt, Maryland 20771

Abstract

A sequential filtering algorithm is presented for attitude and attitude-rate estimation from Global Positioning System (GPS) differential carrier phase measurements. A third-order, minimal-parameter method for solving the attitude matrix kinematic equation is used to parameterize the filter's state, which renders the resulting estimator computationally efficient. Borrowing from tracking theory concepts, the angular acceleration is modeled as an exponentially autocorrelated stochastic process, thus avoiding the use of the uncertain spacecraft dynamic model. The new formulation facilitates the use of aiding vector observations in a unified filtering algorithm, which can enhance the method's robustness and accuracy. Numerical examples are used to demonstrate the performance of the method.

I Introduction

ATTITUDE determination methods using Global Positioning System (GPS) signals have been intensively investigated in recent years. In general, these methods can be classified into two main classes. Point estimation algorithms (also called "deterministic"

*National Research Council Research Associate, Guidance, Navigation and Control Center, Code 571; currently on sabbatical from Department of Aerospace Engineering, Technion—Israel Institute of Technology, Haifa 32000, Israel. Senior Member IEEE. Senior Member AIAA.
Email: *oshman@tx.technion.ac.il.* Tel: (301)286-2228. FAX: (301)286-1718.
†Staff Engineer, Guidance, Navigation and Control Center, Code 571. Fellow AIAA.

algorithms), in which the GPS measurements at each time point are utilized to obtain an attitude solution independently of the solutions at other time points, were introduced, among others, in Refs. 1, 2 and 3. Stochastic filtering algorithms, which process the measurements sequentially and retain the information content of past measurements, can produce better attitude solutions by more effectively filtering the noisy measurements. Such algorithms were recently introduced in Refs. 4 and 5, both of which utilized extended Kalman filtering to sequentially estimate the attitude from GPS carrier phase difference measurements. Both attitude and attitude-rate were estimated, and the filters used the nonlinear Euler equations of motion for attitude propagation. While avoiding the traditional usage of the costly and unreliable gyro package, this approach rendered the resulting filters computationally burdensome and sensitive to inevitable modeling errors.[6] In Ref. 4 an attempt was made to robustify the dynamics-based filter by estimating the unknown disturbance torques, modeled as unknown constants.

Although GPS-based attitude estimation methods should enjoy, in principle, the low price and low power consumption of state-of-the-art GPS receivers, and the general availability and robustness of the global positioning system, these methods are very sensitive to multipath effects and to the geometry of the antennae baseline configuration, and they inherently rely on precise knowledge of the antennae baselines in the spacecraft body frame. On the other hand, methods based on vector observations have reached maturity and popularity in the last three decades. However, as is well known, they too suffer from disadvantages, that can be attributed to the particular attitude sensors on which they are based. Thus, while their readings are relatively noiseless, Sun sensors are very sensitive to Earth radiation effects, and are rendered completely useless during Eclipse. Star trackers can provide accuracy on the order of a few arc-seconds, but are usually extremely expensive. Magnetometers always provide measurements of the Earth magnetic field in spacecraft flying in low Earth orbits, but they are sensitive to unmodeled residual magnetic fields in the spacecraft and to magnetic

field model imperfections and variations.

The method presented herein is a sequential estimator for both the spacecraft attitude matrix and attitude-rate, which mainly uses differential GPS carrier phase measurements, but can also process aiding vector observations (such as low accuracy coarse Sun sensor measurements, or magnetic field measurements). Conceptually similar to the principle of complementary filtering,[7] the idea underlying this estimator is that, due to the different nature of these signals, the combination of both in a unified data processing algorithm can benefit from the relative advantages of both sensor systems, while alleviating the disadvantages of both.

The new estimator is based on a third-order minimal-parameter method for solving the attitude matrix evolution equation using integrated-rate parameters (IRP).[8] Similarly to Refs. 5 and 4, the new estimator is a sequential filtering algorithm and not a deterministic (point estimation) algorithm. However, the new algorithm differs from other works addressing the same problem in two main respects. First, the estimator's propagation model does not utilize the nonlinear Euler equations. Instead, employing an approach borrowed from linear tracking theory,[9] the uncertain dynamic model of the spacecraft is abandoned, and the angular acceleration is modeled as a zero-mean stochastic process with exponential autocorrelation. [A similar, but simpler, approach was employed in the Applied Technology Satellite 6 (ATS-6)[10]]. Combined with the extremely simple evolution equation of the integrated-rate parameters, this results in a simple, linear propagation model. Second, in contrast with other methods relying mainly on the attitude quaternion, the algorithm presented herein directly estimates the attitude matrix, a natural, nonsingular attitude representation. Building upon the minimal, third-order integrated-rate parametrization, the new estimator assigns just three state variables for the parametrization of the nine-parameter attitude matrix, which is at the heart of its computational efficiency.

After a brief review of the IRP method for the solution of the attitude evolution equa-

tion, the angular acceleration kinematic model is presented. Applying minimum mean square error (MMSE) estimation theory to the perturbation model, the measurement processing algorithm is developed for both GPS carrier phase signals and vector observations. An attitude matrix orthogonalization procedure, incorporated to enhance the algorithm's accuracy and robustness, is then introduced, followed by a derivation of the prediction stage. Two numerical examples are then presented, which demonstrate the performance of the new algorithm. Concluding remarks are offered in the last section.

II Integrated-Rate Parameters

Consider the matrix differential equation

$$\dot{V}(t) = W(t)V(t), \qquad V(t_0) = V_0 \tag{1}$$

where $V(t) \in \mathbb{R}^{n,n}$, $W(t) = -W^T(t)$ for all $t \geq t_0$, $V_0 V_0^T = I$ and the overdot indicates the temporal derivative. Defining

$$A(t, t_0) \triangleq \int_{t_0}^{t} W(\tau)\, d\tau \tag{2}$$

$$\bar{W}_0(t) \triangleq W(t) - (t - t_0)\dot{W}(t) \tag{3}$$

it can be shown[11] that the following matrix-valued function is a third-order approximation of $V(t)$:

$$\tilde{V}(t, t_0) \triangleq \left\{ I + A(t, t_0) + \frac{A^2(t, t_0)}{2!} + \frac{A^3(t, t_0)}{3!} + \frac{t - t_0}{3!} \left[A(t, t_0)\bar{W}_0(t) - \bar{W}_0(t)A(t, t_0) \right] \right\} V_0 \tag{4}$$

Moreover, $\tilde{V}$ is a third-order approximation of an orthogonal matrix, i.e., $\tilde{V}(t,t_0)\tilde{V}^T(t,t_0) = I + \mathcal{O}\big((t-t_0)^4\big)$ where $\mathcal{O}(x)$ denotes a function of x that has the property that $\mathcal{O}(x)/x$ is bounded as $x \to 0$.

In the 3-D case, the off-diagonal entries of $A(t,t_0)$, termed integrated-rate parameters, have a simple geometric interpretation: they are the angles resulting from a temporal-integration of the three components of the angular velocity vector

$$\omega(t) \triangleq [\omega_1(t) \quad \omega_2(t) \quad \omega_3(t)]^T \tag{5}$$

where ω_i is the angular velocity component along the i-axis of the initial coordinate system, and $i = 1,2,3$ for x,y,z, respectively. The orthogonal matrix differential equation (1) is rewritten, in this case, as

$$\dot{D}(t) = \Omega(t)D(t), \qquad D(t_0) = D_0 \tag{6}$$

where $D(t)$ is the attitude matrix, or the direction cosine matrix (DCM), $\Omega(t) = -[\omega(t)\times]$, and $[\omega(t)\times]$ is the usual *cross product matrix* corresponding to $\omega(t)$. In this case, the matrix $A(t,t_0)$ takes the form

$$A(t,t_0) \triangleq -[\theta(t)\times] \tag{7}$$

where the parameter vector $\theta(t)$ is defined as

$$\theta(t) \triangleq \Big[\theta_1(t) \quad \theta_2(t) \quad \theta_3(t)\Big]^T \tag{8}$$

and

$$\theta_i(t) \triangleq \int_{t_0}^{t} \omega_i(\tau)\, d\tau, \qquad i = 1, 2, 3 \tag{9}$$

Let the sampling period be denoted by $T \triangleq t_{k+1} - t_k$. Using the notation $\theta(k) \triangleq \theta(t_k)$, the parameter vector at time t_k is $\theta(k) = [\theta_1(k) \quad \theta_2(k) \quad \theta_3(k)]^T$ and Eq. (9) implies

$$\theta_i(k) = \int_{t_0}^{t_k} \omega_i(\tau)\, d\tau, \qquad i = 1, 2, 3 \tag{10}$$

From Eq. (10) we have

$$\theta(k+1) = \theta(k) + \int_{t_k}^{t_{k+1}} \omega(\tau)\, d\tau \tag{11}$$

Define $A(k+1, k)$ to be the discrete-time analog of $A(t, t_0)$, i.e.,

$$A(k+1, k) \triangleq -\big[\big(\theta(k+1) - \theta(k)\big)\times\big] \tag{12}$$

Also, let $\Psi(k+1) \triangleq -\big[\psi(k+1)\times\big]$, where

$$\psi(k+1) \triangleq \omega(k+1) - \dot{\omega}(k+1)T \tag{13}$$

Then, the corresponding discrete-time equivalent of Eq. (4) is

$$D(k+1) = \Big\{ I + A(k+1, k) + \frac{1}{2}A^2(k+1, k) + \frac{1}{6}A^3(k+1, k) + \frac{1}{6}T\Big[A(k+1, k)\Psi(k+1) - \Psi(k+1)A(k+1, k)\Big]\Big\} D(k) \tag{14}$$

which, using Eqs. (12) and (13), can be written as

$$D(k+1) = D\big[\theta(k+1) - \theta(k), \omega(k+1), \dot{\omega}(k+1), D(k)\big] \tag{15}$$

III Kinematic Motion Model

To avoid using the uncertain spacecraft dynamic model, the spacecraft angular acceleration is modeled as a zero-mean stochastic process with exponential autocorrelation function. The acceleration dynamic model is, therefore, the following first-order Markov process,

$$\ddot{\omega}(t) = -\Lambda\dot{\omega}(t) + \tilde{\nu}(t) \tag{16}$$

For simplicity, a decoupled kinematic model is chosen for the three angular rate components, i.e., $\Lambda \triangleq \text{diag}\{\tau_1^{-1}, \tau_2^{-1}, \tau_3^{-1}\}$, where $\{\tau_i\}_{i=1}^3$ are the acceleration decorrelation times associated with the corresponding body axes. The driving noise is a zero-mean white process, with power spectral density (PSD) matrix

$$\tilde{Q}(t) = 2\Lambda\Sigma^2, \qquad \Sigma \triangleq \text{diag}\{\sigma_1, \sigma_2, \sigma_3\} \tag{17}$$

The noise variances in Eq. (17) were chosen according to the Singer angular acceleration probabilistic model,[9] in which the angular acceleration components, $\{\dot{\omega}_i\}_{i=1}^3$, can be 1) equal to $\dot{\omega}_{Mi}$ with probability p_{Mi}, 2) equal to $-\dot{\omega}_{Mi}$ with probability p_{Mi}, 3) equal to zero with probability p_{0i}, or 4) uniformly distributed over the interval $[-\dot{\omega}_{Mi}, \dot{\omega}_{Mi}]$ with the remaining probability mass. Using this model, it follows that

$$\sigma_i^2 = \frac{\dot{\omega}_{Mi}^2}{3}(1 + 4p_{Mi} - p_{0i}) \tag{18}$$

The parameters $\dot{\omega}_{M_i}$, p_{M_i} and p_{0_i} are considered as filter tuning parameters. As customarily done, they are selected by experience with real and simulated data, so as to optimally adapt the filter to the characteristics of the problem at hand.

Defining now the system's state vector as

$$x(t) \triangleq \left[\theta^T(t) \quad \omega^T(t) \quad \dot{\omega}^T(t)\right]^T \tag{19}$$

the state equation is

$$\dot{x}(t) = Fx(t) + \tilde{v}(t) \equiv \begin{bmatrix} 0 & I & 0 \\ 0 & 0 & I \\ 0 & 0 & -\Lambda \end{bmatrix} x(t) + \begin{bmatrix} 0 \\ 0 \\ \tilde{\nu}(t) \end{bmatrix} \tag{20}$$

with obvious definitions of F and $\tilde{v}(t)$. Corresponding to the sampling interval T, the discrete-time state equation is

$$x(k+1) = \Phi(T)x(k) + v(k) \tag{21}$$

where the transition matrix is

$$\Phi(T) \equiv e^{FT} = \begin{bmatrix} I & TI & \Lambda^{-2}\left(e^{-\Lambda T} - I + T\Lambda\right) \\ 0 & I & \Lambda^{-1}\left(I - e^{-\Lambda T}\right) \\ 0 & 0 & e^{-\Lambda T} \end{bmatrix} \tag{22}$$

and $v(k)$ is a zero-mean, white noise sequence, with covariance matrix

$$Q(k) \triangleq E\{v(k)v^T(k)\} = \int_0^T e^{F(T-t)}\mathrm{diag}\left\{0, 0, \tilde{Q}(t)\right\}e^{F^T(T-t)}\,dt \tag{23}$$

Explicit computation of the integrals in Eq. (23) yields the following expressions for the

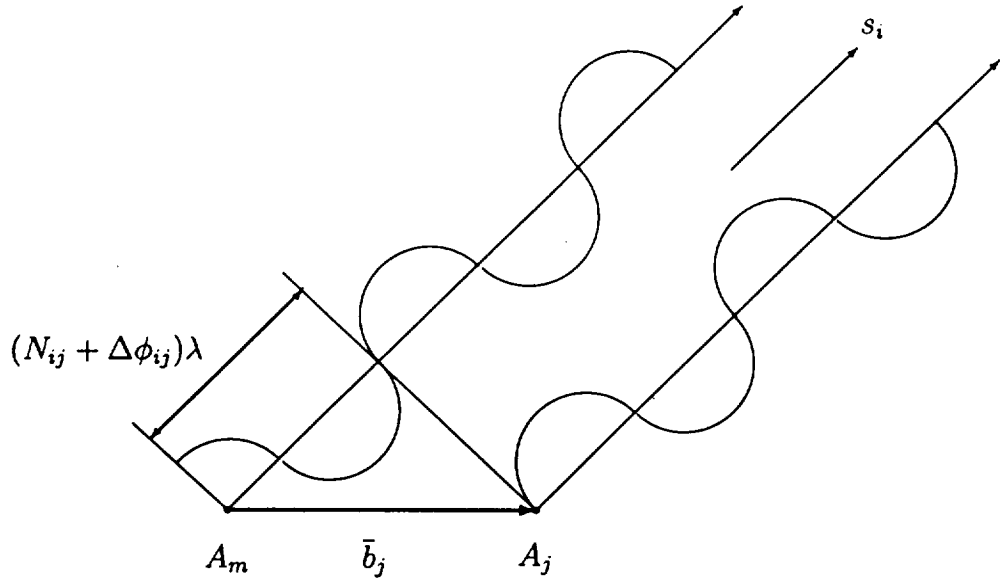

Fig. 1: GPS Phase Difference Measurement Geometry

entries of the symmetric covariance matrix $Q(k)$

$$Q_{11}(k) = \Lambda^{-4}\Sigma^2\left(I + 2\Lambda T - 2\Lambda^2T^2 + \frac{2}{3}\Lambda^3T^3 - e^{-2\Lambda T} - 4\Lambda Te^{-\Lambda T}\right) \tag{24a}$$

$$Q_{12}(k) = \Lambda^{-3}\Sigma^2\left(I - 2\Lambda T + \Lambda^2T^2 - 2e^{-\Lambda T} + e^{-2\Lambda T} + 2\Lambda Te^{-\Lambda T}\right) \tag{24b}$$

$$Q_{13}(k) = \Lambda^{-2}\Sigma^2\left(I - e^{-2\Lambda T} - 2\Lambda Te^{-\Lambda T}\right) \tag{24c}$$

$$Q_{22}(k) = \Lambda^{-2}\Sigma^2\left(4e^{-\Lambda T} - 3I - e^{-2\Lambda T} + 2\Lambda T\right) \tag{24d}$$

$$Q_{23}(k) = \Lambda^{-1}\Sigma^2\left(e^{-2\Lambda T} + I - 2e^{-\Lambda T}\right) \tag{24e}$$

$$Q_{33}(k) = \Sigma^2\left(I - e^{-2\Lambda T}\right) \tag{24f}$$

IV Measurement Processing

GPS Differential Phase Measurements

Consider the basic GPS antenna array, depicted in Fig. 1. The array consists of the master antenna, A_m, and the slave antenna, A_j. These antennas are located on the satellite's surface,

such that the baseline vector between them, resolved in a body-fixed coordinate system, is $\bar{b}_j$. It is assumed that the entire system consists of m_b antennas, in addition to the master antenna, so that there exist m_b independent baselines. It is also assumed that at time t_{k+1}, m_s GPS satellites are in view.

Consider the ith satellite, and denote the sightline (unit) direction vector to that satellite, resolved in an inertial coordinate system, by s_i. Let $D(k+1)$ be the attitude matrix transforming vectors in the inertial coordinate system to their body-fixed system representations at time t_{k+1}. Let $N_{ij}(k+1)$ and $\Delta\phi_{ij}(k+1)$ denote the integer and fractional parts, respectively, of the phase difference between the two carrier signals, corresponding to the ith satellite, as acquired by the antennas A_m and A_j. Denoting by λ the GPS carrier wavelength, the true (noiseless) signals satisfy

$$\big[\Delta\phi_{ij}(k+1) + N_{ij}(k+1)\big]\lambda = \bar{b}_j^T D(k+1)s_i \tag{25}$$

The standard GPS carrier wavelength is 19.03 cm. In this work, it is assumed that the integer part of the phase difference between the two receivers is known from a previous solution.[1,12]

In practice, the phase measurements will be contaminated by noise, the primary source of which is due to the multipath effect.[1] Denoting the noise corresponding to the baseline $\bar{b}_j$ and the sightline s_i by $\tilde{n}_{ij}(k+1)$, the real measurement equation is

$$\big[\Delta\phi_{ij}(k+1) + N_{ij}(k+1)\big]\lambda = \bar{b}_j^T D(k+1)s_i + \tilde{n}_{ij}(k+1) \tag{26}$$

where it is assumed that $\tilde{n}_{ij}(k+1) \sim \mathcal{N}\big(0, \tilde{\sigma}_{ij}^2(k+1)\big)$. Typically it can be assumed that the noise standard deviation is on the order of 5 mm.[1] From Eq. (26) we obtain the normalized measurement equation

$$\Delta\phi_{ij}(k+1) + N_{ij}(k+1) = b_j^T D(k+1)s_i + n_{ij}(k+1) \tag{27}$$

where we have defined $b_j \triangleq \bar{b}_j/\lambda$ and $n_{ij}(k+1) \triangleq \tilde{n}_{ij}(k+1)/\lambda$. The normalized measurement noise satisfies $n_{ij}(k+1) \sim \mathcal{N}\big(0, \sigma_{ij}^2(k+1)\big)$, where

$$\sigma_{ij}(k+1) = \tilde{\sigma}_{ij}(k+1)/\lambda. \tag{28}$$

GPS Measurement Linearization

At t_{k+1} the minimum mean square error (MMSE) predicted vector is $\hat{x}(k+1|k)$, and its corresponding prediction error covariance matrix is $P(k+1|k) \triangleq E\{\tilde{x}(k+1|k)\tilde{x}^T(k+1|k)\}$, where the estimation error is

$$\tilde{x}(j|k) \triangleq x(j) - \hat{x}(j|k). \tag{29}$$

Using Eq. (15), Eq. (27) is rewritten as

$$N_{ij}(k+1) + \Delta\phi_{ij}(k+1) = b_j^T D\big[\theta(k+1) - \theta(k), \omega(k+1), \dot{\omega}(k+1), D(k)\big]s_i + n_{ij}(k+1) \tag{30}$$

Next, we linearize the nonlinear measurement equation (30) about the most recent estimate at t_{k+1}, i.e.,

$$x(k+1) = \hat{x}(k+1|k) + \delta x(k+1) \equiv \begin{bmatrix} \hat{\theta}(k+1|k) \\ \hat{\omega}(k+1|k) \\ \hat{\dot{\omega}}(k+1|k) \end{bmatrix} + \begin{bmatrix} \delta\theta(k+1) \\ \delta\omega(k+1) \\ \delta\dot{\omega}(k+1) \end{bmatrix} \tag{31}$$

where $\delta\theta(k+1)$, $\delta\omega(k+1)$ and $\delta\dot{\omega}(k+1)$ are the perturbations of the state components about the nominal (i.e., predicted) state. Let $\hat{D}^*(k|k)$ denote the a posteriori, *orthogonalized* estimate of the attitude matrix at time t_k, to be discussed in the next section. Using now the most recent estimates for $D(k)$ and $x(k)$, namely $\hat{D}^*(k|k)$ and $\hat{x}(k|k)$, respectively, in

Eq. (30), it follows that

$$\Delta\phi_{ij}(k+1) + N_{ij}(k+1) = b_j^T D\big[\hat{\theta}(k+1|k) + \delta\theta(k+1) - \hat{\theta}(k|k), \hat{\omega}(k+1|k) + \delta\omega(k+1), \hat{\omega}(k+1|k) + \delta\dot{\omega}(k+1), \hat{D}^*(k|k)\big] s_i + n_{ij}(k+1) \tag{32}$$

As discussed in the sequel, the a posteriori IRP estimate is zeroed after each measurement update (due to full reset control of the IRP state). We will, therefore, use the reset value of the IRP estimate, $\hat{\theta}^c(k|k) = 0$, in Eq. (32). Now expand D about the nominal state using a first-order Taylor series expansion, i.e.,

$$\begin{aligned}
&D\big[\hat{\theta}(k+1|k) + \delta\theta(k+1), \hat{\omega}(k+1|k) + \delta\omega(k+1), \hat{\dot{\omega}}(k+1|k) + \delta\dot{\omega}(k+1), \hat{D}^*(k|k)\big] \\
&\quad = \hat{D}(k+1|k) + \sum_{i=1}^{3} \frac{\partial D\big[\theta(k+1), \hat{\omega}(k+1|k), \hat{\dot{\omega}}(k+1|k), \hat{D}^*(k|k)\big]}{\partial\theta_i}\Big|_{\hat{\theta}(k+1|k)} \delta\theta_i(k+1) \\
&\quad + \sum_{i=1}^{3} \frac{\partial D\big[\hat{\theta}(k+1|k), \omega(k+1), \hat{\dot{\omega}}(k+1|k), \hat{D}^*(k|k)\big]}{\partial\omega_i}\Big|_{\hat{\omega}(k+1|k)} \delta\omega_i(k+1) \\
&\quad + \sum_{i=1}^{3} \frac{\partial D\big[\hat{\theta}(k+1|k), \hat{\omega}(k+1|k), \dot{\omega}(k+1), \hat{D}^*(k|k)\big]}{\partial\dot{\omega}_i}\Big|_{\hat{\dot{\omega}}(k+1|k)} \delta\dot{\omega}_i(k+1)
\end{aligned} \tag{33}$$

where $(\bullet)\big|_{\zeta}$ denotes 'evaluated at ζ' and

$$\hat{D}(k+1|k) \triangleq D\big[\hat{\theta}(k+1|k), \hat{\omega}(k+1|k), \hat{\dot{\omega}}(k+1|k), \hat{D}^*(k|k)\big] \tag{34}$$

Differentiating Eq. (14), the sensitivity matrices appearing in Eq. (33) are computed as

$$\frac{\partial}{\partial\theta_i} D\big[\theta(k+1), \hat{\omega}(k+1|k), \hat{\dot{\omega}}(k+1|k), \hat{D}^*(k|k)\big] = G_i\big[\theta(k+1), \hat{\psi}(k+1|k)\big]\hat{D}^*(k|k) \tag{35a}$$

$$\frac{\partial}{\partial\omega_i} D\big[\hat{\theta}(k+1|k), \omega(k+1), \hat{\dot{\omega}}(k+1|k), \hat{D}^*(k|k)\big] = \frac{1}{6}TF_i\big[\hat{\theta}(k+1|k)\big]\hat{D}^*(k|k) \tag{35b}$$

$$\frac{\partial}{\partial\dot{\omega}_i} D\big[\hat{\theta}(k+1|k), \hat{\omega}(k+1|k), \dot{\omega}(k+1), \hat{D}^*(k|k)\big] = -\frac{1}{6}T^2F_i\big[\hat{\theta}(k+1|k)\big]\hat{D}^*(k|k) \tag{35c}$$

for $i = 1, 2, 3$, where

$$\hat{\psi}(k+1|k) \triangleq \hat{\omega}(k+1|k) - T\hat{\dot{\omega}}(k+1|k) \tag{36}$$

and

$$G_i(\theta, \psi) = \frac{1}{2}(\theta e_i^T + e_i\theta^T) - \theta_i I - (1 - \frac{1}{6}\|\theta\|^2)[e_i\times] + \frac{1}{6}T(\psi e_i^T - e_i\psi^T) + \frac{1}{3}\theta_i[\theta\times] \tag{37a}$$

$$F_i(\theta) = e_i\theta^T - \theta e_i^T \tag{37b}$$

where e_i is the unit vector on the ith axis, $i = 1, 2, 3$.

Using Eqs. (33), (35) and (37) in Eq. (32) yields

$$\Delta\phi_{ij}(k+1) + N_{ij}(k+1) - b_j^T\hat{D}(k+1|k)s_i = h_{ij}^T(k+1)\delta x(k+1) + n_{ij}(k+1) \tag{38}$$

where the observation vector $h_{ij}(k+1) \in \mathbb{R}^9$ is defined as

$$h_{ij}(k+1) \equiv \left[h_{\theta_{ij}}^T(k+1) \quad h_{\omega_{ij}}^T(k+1) \quad h_{\dot{\omega}_{ij}}^T(k+1)\right]^T \tag{39}$$

and the elements of the vectors $h_{\theta ij}(k+1) \in \mathbb{R}^3$, $h_{\omega ij}(k+1) \in \mathbb{R}^3$ and $h_{\dot{\omega} ij}(k+1) \in \mathbb{R}^3$ are

$$h_{\theta ij_p}(k+1) = b_j^T G_p[\hat{\theta}(k+1|k), \hat{\psi}(k+1|k)]\hat{D}^*(k|k)s_i, \qquad p = 1, 2, 3 \tag{40a}$$

$$h_{\omega ij_p}(k+1) = \frac{1}{6}Tb_j^T F_p[\hat{\theta}(k+1|k)]\hat{D}^*(k|k)s_i, \qquad p = 1, 2, 3 \tag{40b}$$

$$h_{\dot{\omega} ij_p}(k+1) = -Th_{\omega ij_p}(k+1), \qquad p = 1, 2, 3 \tag{40c}$$

Define now the *effective* GPS measurement to be

$$y_{ij}^{\phi}(k+1) \triangleq \Delta\phi_{ij}(k+1) + N_{ij} - b_j^T\hat{D}(k+1|k)s_i \tag{41}$$

Then, using this definition in Eq. (38) yields the following scalar measurement equation:

$$y_{ij}^{\phi}(k+1) = {h_{ij}}^{T}(k+1)\delta x(k+1) + n_{ij}(k+1) \tag{42}$$

For the m_b baselines and m_s sightlines, there exist $m_s \times m_b$ scalar measurements like Eq. (42). We next aggregate all of these equations into a single vector equation, such that the measurement associated with the baseline b_j and sightline s_i corresponds to the pth component of the vector measurement equation, where $p = (j-1)m_s + i$. This yields

$$y^{\phi}(k+1) = H^{\phi}(k+1)\delta x(k+1) + n^{\phi}(k+1) \tag{43}$$

where the pth row of the matrix $H^{\phi}(k+1)$ is ${h_{ij}}^{T}(k+1)$, the measurement noise satisfies

$$n^{\phi}(k+1) \sim \mathcal{N}\big(0, R^{\phi}(k+1)\big) \tag{44}$$

and the covariance $R^{\phi}(k+1)$ is a diagonal matrix whose diagonal elements are

$$R_{pp}^{\phi}(k+1) = \sigma_{ij}^{2} \tag{45}$$

Vector Observation Aiding

If the sole source of attitude information is the GPS carrier phase signals, then Eq. (43) should serve as the basis for the development of the measurement update algorithm (in the next section). In the case that vector observations are available, this information structure needs to be augmented.

Assume that a new pair of corresponding noisy vector measurements is acquired at t_{k+1}. This pair consists of the *unit* vectors $u(k+1)$ and $v(k+1)$, which represent the values of the same vector $r(k+1)$, as modeled in the reference coordinate system and measured in

the body coordinate system, respectively. The direction-cosine matrix $D(k+1)$ transforms the *true* vector representation u_0 into its corresponding *true* representation v_0 according to

$$v_0(k+1) = D(k+1)u_0(k+1) \tag{46}$$

Assuming no constraint on the measurement noise direction, the body-frame measured unit vector, $v(k+1)$, is related to the true vector according to

$$v(k+1) = \frac{v_0(k+1) + n'_v(k+1)}{\|v_0(k+1) + n'_v(k+1)\|} \tag{47}$$

where the white sensor measurement noise is $n'_v(k+1) \sim \mathcal{N}\big(0, R'_v(k+1)\big)$. Since both $v_0(k+1)$ and $v(k+1)$ are unit vectors, it follows from Eq. (47) that

$$v(k+1) = v_0(k+1) + n_v(k+1) \tag{48}$$

where $n_v(k+1) \triangleq \mathcal{P}^{\perp}_{v_0}(k+1)n'_v(k+1)$ and $\mathcal{P}^{\perp}_{v_0}(k+1) \triangleq I - v_0(k+1)v_0^T(k+1)$ is the orthogonal projector onto the orthogonal complement of span$\big\{v_0(k+1)\big\}$. To a good approximation, the effective measurement noise is a zero mean, white Gaussian sequence with covariance

$$R_v(k+1) = \mathcal{P}^{\perp}_{v_0}(k+1)R'_v(k+1)\mathcal{P}^{\perp}_{v_0}(k+1) \tag{49}$$

To account for non-ideal effects (e.g., star catalog errors), it is assumed that the modeled reference vector is related to the true vector according to

$$u(k+1) = u_0(k+1) + n_u(k+1) \tag{50}$$

where $n_u \perp u_0$ is a zero mean, white Gaussian noise, that is uncorrelated with n_v and has a known covariance matrix $R_u(k)$.

Vector Measurement Linearization

Using Eq. (15), Eq. (46) can be rewritten as

$$v_0(k+1) = D\big[\theta(k+1) - \theta(k), \omega(k+1), \dot{\omega}(k+1), D(k)\big] u_0(k+1) \tag{51}$$

Linearizing about the predicted estimates and using Eqs. (31), (48) and (50), it follows that

$$\begin{aligned} v(k+1) - n_v(k+1) = D\big[&\hat{\theta}(k+1|k) + \delta\theta(k+1), \hat{\omega}(k+1|k) + \delta\omega(k+1), \\ &\hat{\dot{\omega}}(k+1|k) + \delta\dot{\omega}(k+1), \hat{D}^*(k|k)\big]\big[u(k+1) - n_u(k+1)\big] \end{aligned} \tag{52}$$

where, as previously done in the GPS measurement linearization, the reset value of the IRP estimate, $\hat{\theta}^c(k|k) = 0$, has been used. Expanding D about the nominal state using the first-order Taylor series (33) yields

$$\begin{aligned} v(k+1) - \hat{D}(k+1|k)u(k+1) &= \sum_{i=1}^{3}\Big[G_i\big[\hat{\theta}(k+1|k), \hat{\psi}(k+1|k)\big]\delta\theta_i(k+1) \\ &+ \frac{1}{6}TF_i\big[\hat{\theta}(k+1|k)\big]\delta\omega_i(k+1) - \frac{1}{6}T^2F_i\big[\hat{\theta}(k+1|k)\big]\delta\dot{\omega}_i(k+1)\Big]\hat{D}^*(k|k)u(k+1) \\ &- \hat{D}(k+1|k)n_u(k+1) + n_v(k+1) \\ &= H^v(k+1)\delta x(k+1) - \hat{D}(k+1|k)n_u(k+1) + n_v(k+1) \end{aligned} \tag{53}$$

where the observation matrix $H^v(k+1)$ is written in block matrix form as

$$H^v(k+1) \equiv \begin{bmatrix} H_1(k+1) & H_2(k+1) & H_3(k+1) \end{bmatrix} \tag{54}$$

and the columns of the submatrices $H_i(k+1) \in \mathbb{R}^{3,3}$, $i = 1, 2, 3$ are

$$H_{1j}(k+1) = G_j\left[\hat{\theta}(k+1|k), \hat{\psi}(k+1|k)\right]\hat{D}^*(k|k)u(k+1) \tag{55a}$$

$$H_{2j}(k+1) = \frac{1}{6}TF_j\left[\hat{\theta}(k+1|k)\right]\hat{D}^*(k|k)u(k+1) \tag{55b}$$

$$H_{3j}(k+1) = -TH_{2j}(k+1) \tag{55c}$$

for $j = 1, 2, 3$. Notice that the same sensitivity matrices are used here, as in the linearized GPS measurement equation, which implies obvious computational saving. Define now the *effective* measurement and measurement noise to be, respectively,

$$y^\nu(k+1) \triangleq v(k+1) - \hat{D}(k+1|k)u(k+1) \tag{56}$$

$$n^\nu(k+1) \triangleq n_v(k+1) - \hat{D}(k+1|k)n_u(k+1) \tag{57}$$

Then, using these definitions in Eq. (53) yields the following measurement equation:

$$y^\nu(k+1) = H^\nu(k+1)\delta x(k+1) + n^\nu(k+1) \tag{58}$$

where $n^\nu(k+1) \sim \mathcal{N}\big(0, R^\nu(k+1)\big)$ is the white measurement noise, and

$$R^\nu(k+1) \triangleq R_v(k+1) + \hat{D}(k+1|k)R_u(k+1)\hat{D}^T(k+1|k) \tag{59}$$

Measurement Update

To process the measurements, define now

$$y \triangleq \begin{bmatrix} y^\phi \\ y^\nu \end{bmatrix}, \qquad H \triangleq \begin{bmatrix} H^\phi \\ H^\nu \end{bmatrix}, \qquad n \triangleq \begin{bmatrix} n^\phi \\ n^\nu \end{bmatrix} \tag{60}$$

where $n \sim \mathcal{N}(0, R)$ and $R \triangleq \text{diag}\{R^{\phi}, R^{\nu}\}$. Since

$$\delta x(k+1) = x(k+1) - \hat{x}(k+1|k) = \tilde{x}(k+1|k) \tag{61}$$

and $\hat{x}(k+1|k)$ is an unbiased, MMSE predictor, we have

$$E\{\delta x(k+1)\} = E\{\tilde{x}(k+1|k)\} = 0 \tag{62}$$

and

$$\text{cov}\{\delta x(k+1)\} = \text{cov}\{\tilde{x}(k+1|k)\} = P(k+1|k) \tag{63}$$

thus

$$\delta x(k+1) \sim \mathcal{N}(0, P(k+1|k)) \tag{64}$$

Using the linearized measurement equation and the statistical properties of the measurement and prediction errors, the MMSE estimator of $\delta x(k+1)$ is

$$\widehat{\delta x}(k+1|k+1) = K(k+1)y(k+1) \tag{65}$$

where $K(k+1)$, the estimator gain matrix, is computed as

$$K(k+1) = P(k+1|k)H^T(k+1)\left[H(k+1)P(k+1|k)H^T(k+1) + R(k+1)\right]^{-1} \tag{66}$$

Also, $\widehat{\delta x}(k+1|k+1) = \hat{x}(k+1|k+1) - \hat{x}(k+1|k)$ which, used in Eq. (65), yields the state measurement update equation

$$\hat{x}(k+1|k+1) = \hat{x}(k+1|k) + K(k+1)y(k+1) \tag{67}$$

Subtracting $x(k+1)$ from both sides of the last equation yields

$$\tilde{x}(k+1|k+1) = \big[I - K(k+1)H(k+1)\big]\tilde{x}(k+1|k) - K(k+1)n(k+1) \tag{68}$$

from which the resulting covariance update equation is

$$\begin{aligned} P(k+1|k+1) = {} & \big[I - K(k+1)H(k+1)\big]P(k+1|k)\big[I - K(k+1)H(k+1)\big]^T \\ & + K(k+1)R(k+1)K^T(k+1) \end{aligned} \tag{69}$$

where the filtering error covariance is $P(k+1|k+1) \triangleq E\{\tilde{x}(k+1|k+1)\tilde{x}^T(k+1|k+1)\}$.

To compute the measurement-updated attitude matrix at time t_{k+1}, we use the most recent estimate $\hat{x}(k+1|k+1)$ and the estimated attitude matrix corresponding to time t_k in Eq. (14). This yields

$$\begin{aligned} \hat{D}(k+1|k+1) = {} & \Big\{ I + \hat{A}(k+1,k) + \frac{1}{2}\hat{A}^2(k+1,k) + \frac{1}{6}\hat{A}^3(k+1,k) \\ & + \frac{1}{6}T\Big[\hat{A}(k+1,k)\hat{\Psi}(k+1|k+1) - \hat{\Psi}(k+1|k+1)\hat{A}(k+1,k)\Big]\Big\}\hat{D}^*(k|k) \end{aligned} \tag{70}$$

where the *a posteriori* estimates of $A(k+1,k)$ and $\Psi(k+1)$ are defined, respectively, as

$$\hat{A}(k+1,k) \triangleq -\big[\hat{\theta}(k+1|k+1)\times\big] \tag{71}$$

$$\hat{\Psi}(k+1|k+1) \triangleq -\big[\hat{\psi}(k+1|k+1)\times\big] \tag{72}$$

where

$$\hat{\psi}(k+1|k+1) \triangleq \hat{\omega}(k+1|k+1) - T\hat{\omega}(k+1|k+1) \tag{73}$$

and $\hat{D}^{\bullet}(k|k)$ is the a posteriori, *orthogonalized* estimate of the attitude matrix at time t_k, to be discussed in the next section.

Finally, since the a posteriori attitude matrix, $\hat{D}(k+1|k+1)$, is computed based on the a posteriori estimate, $\hat{\theta}(k+1|k+1)$, this implies a full *reset control* [13, p. 332] of the parameter vector, i.e.,

$$\theta^{c}(k+1) = \theta(k+1) - \hat{\theta}(k+1|k+1) \tag{74}$$

where $\theta^{c}(k+1)$ is the *reset* state vector at t_{k+1}, and a corresponding reset of the state estimate,

$$\hat{\theta}^{c}(k+1|k+1) = 0 \tag{75}$$

which is then used in the ensuing time propagation step. Since the reset control is applied to *both* the state vector and its estimate, no changes are necessary in the estimation error covariance matrix.

V Attitude Matrix Orthogonalization

To improve the algorithm's accuracy and enhance its stability, an additional orthogonalization procedure is introduced into the estimator, following the measurement update stage. In this procedure, the attitude matrix closest to the filtered attitude matrix is computed.

Given the filtered attitude matrix $\hat{D}(k+1|k+1)$, the attitude matrix orthogonalization

problem is to find the matrix

$$\hat{D}^*(k+1|k+1) \triangleq \arg \min_{D \in \mathbb{R}^{3,3}} \left\| \hat{D}(k+1|k+1) - D \right\| \tag{76a}$$

subject to

$$D^T D = I \qquad \text{and} \qquad \det D = +1 \tag{76b}$$

Being a special case of the orthogonal Procrustes problem,[14] the matrix orthogonalization problem can be easily solved using the singular value decomposition (SVD).[15] Thus, if

$$\hat{D}(k+1|k+1) = U(k+1)\Sigma(k+1)V^T(k+1) \tag{77}$$

is the SVD of the matrix $\hat{D}(k+1|k+1)$ where $U(k+1)$ and $V(k+1)$ are the left and right singular vector matrices, respectively, and $\Sigma(k+1) = \text{diag}\{s_1, s_2, s_3\}$ is the singular value matrix where $s_1 \geq s_2 \geq s_3$, then

$$\hat{D}^*(k+1|k+1) = U(k+1)\text{diag}\{1, 1, \det U(k+1) \det V(k+1)\}V^T(k+1) \tag{78}$$

In real-time attitude determination and control the excessive computational burden associated with the SVD might render its use prohibitive. In such cases, the following approximate orthogonalization method, consisting of a single-step application of the iterative method introduced in Ref. 16, can be utilized:

$$\hat{D}^*(k+1|k+1) = N(k+1)\hat{D}(k+1|k+1) \tag{79}$$

where

$$N(k+1) \triangleq \frac{3}{2}I - \frac{1}{2}\hat{D}(k+1|k+1)\hat{D}^T(k+1|k+1) \tag{80}$$

Remark 1. Using an approach similar to that used in Ref. 17, it can be shown that, to first-order, the orthogonalization procedure does not affect the statistical properties of the estimator and, therefore, does not necessitate any adjustments in the algorithm.

VI Prediction

In the prediction step at t_k, the reset a posteriori estimate at time t_k, $\hat{x}^c(k|k)$ (computed with the reset IRP estimate) and its corresponding error covariance matrix, $P(k|k)$, are propagated to time t_{k+1}.

Using Eq. (21), we have

$$\hat{x}(k+1|k) = \Phi(T)\hat{x}^c(k|k) \tag{81}$$

Using this result with Eq. (21) yields the covariance propagation equation

$$P(k+1|k) = \Phi(T)P(k|k)\Phi^T(T) + \Gamma(T)Q(k)\Gamma^T(T) \tag{82}$$

To propagate the attitude matrix to t_{k+1} we use the most recent IRP, attitude-rate and angular acceleration estimates, and the orthogonalized DCM estimate corresponding to t_k, in Eq. (14). This yields

$$\hat{D}(k+1|k) = \left\{ I + \bar{A}(k+1,k) + \frac{1}{2}\bar{A}^2(k+1,k) + \frac{1}{6}\bar{A}^3(k+1,k) \right.$$
$$\left. + \frac{1}{6}T\left[\bar{A}(k+1,k)\hat{\Psi}(k+1|k) - \hat{\Psi}(k+1|k)\bar{A}(k+1,k)\right] \right\} \hat{D}^*(k|k) \tag{83}$$

where the *a priori* estimates of $A(k+1,k)$ and $\Psi(k+1)$ are defined, respectively, as

$$\bar{A}(k+1,k) \triangleq -\left[\hat{\theta}(k+1|k)\times\right] \tag{84}$$

$$\hat{\Psi}(k+1|k) \triangleq -\left[\hat{\psi}(k+1|k)\times\right] \tag{85}$$

VII Numerical Study

Two numerical examples are presented in this section, to demonstrate the performance of the new estimator, and illustrate the performance enhancement achieved by using aiding vector observations.

Example I

In this example, three non-orthogonal baselines were used: $\bar{b}_1 = \left[1.0,\ 1.0,\ 0.0\right]^T$, $\bar{b}_2 = \left[0.0,\ 1.0,\ 0.0\right]^T$, $\bar{b}_3 = \left[0.0,\ 0.0,\ 1.0\right]^T$. Two fixed sightlines were observed at all times, $s_1 = \frac{1}{\sqrt{3}}\left[1.0,\ 1.0,\ 1.0\right]^T$ and $s_2 = \frac{1}{\sqrt{2}}\left[0.0,\ 1.0,\ 1.0\right]^T$. The non-normalized GPS signal noise standard deviation was 5.0 mm. When vector measurements were used, the noise equivalent angle of the inertially-referenced observations was set to 5.0 arc-s, while the body-referenced vector measurements were simulated to be acquired by a low accuracy attitude sensor with a noise equivalent angle of 0.1 deg. These measurements corresponded to a randomly selected vector, which was kept constant throughout the run.

The angular rates of the satellite satisfied $\omega_i(t) = A_i \sin(\frac{2\pi}{T_i}t + \phi_i)$, where the amplitudes A_i are 0.02, 0.05 and 0.03 deg/s, the phases ϕ_i are $\pi/4$, $\pi/2$ and $3\pi/4$ rad, and the periods T_i are 85, 45 and 65 s for $i = 1, 2, 3$, respectively. The initial angular rate estimates were all set to zero. The true initial attitude corresponded to Euler angles of 30 deg, 20 deg and 10 deg in roll, pitch and yaw, respectively, while the filter's initial state corresponded to Euler angles of 25 deg, 15 deg and 5 deg, respectively. The filter was run at a rate of 20 Hz,

and the measurement processing rate was 10 Hz. The Singer angular acceleration model was used with parameters set to $\tau = 10$ s, $\dot{\omega}_M = 10^{-4}$ rad/s^2, $p_M = p_0 = .001$ for all three axes.

In Fig. 2, the three true Euler angles are shown for a typical run. These angles were computed from the true attitude matrix assuming a 3-2-1 angle sequence. The Euler angle

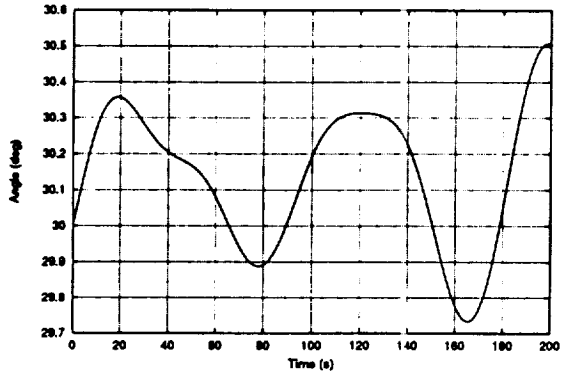

(a) Roll angle

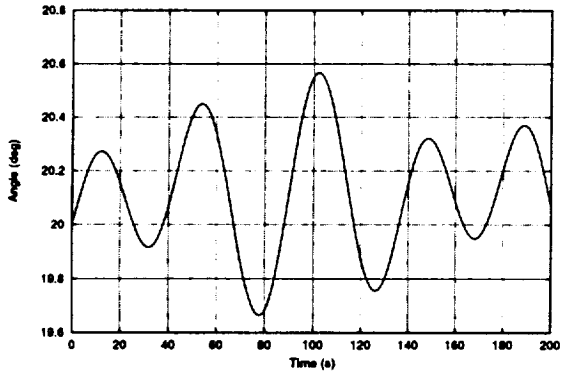

(b) Pitch angle

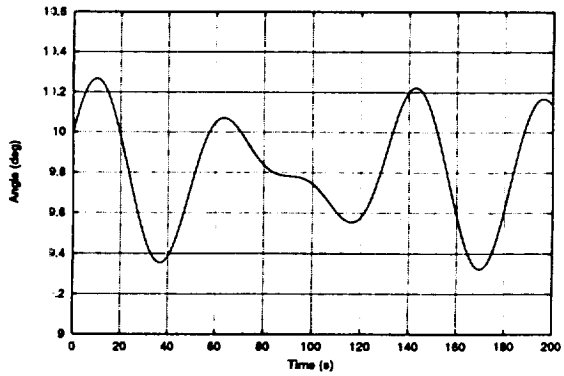

(c) Yaw angle

Fig. 2: Example I: True Euler angles.

estimation errors, computed from the estimated attitude matrix assuming a 3-2-1 Euler angle sequence, are shown in Fig. 3. Fig. 4 presents the angular rates estimation errors for the same run, with and without vector measurement aiding. The mean and standard deviation of the estimation errors are summarized in Table 1, which demonstrates the effect of the

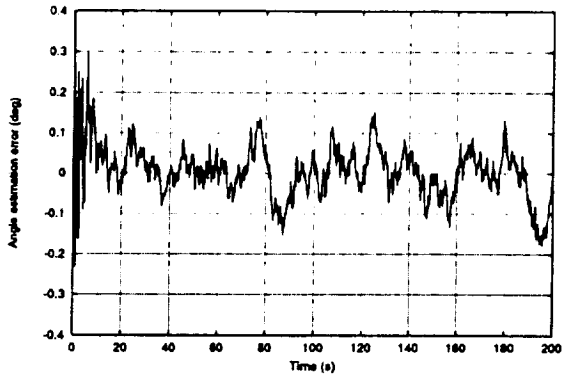

(a) Roll – GPS only

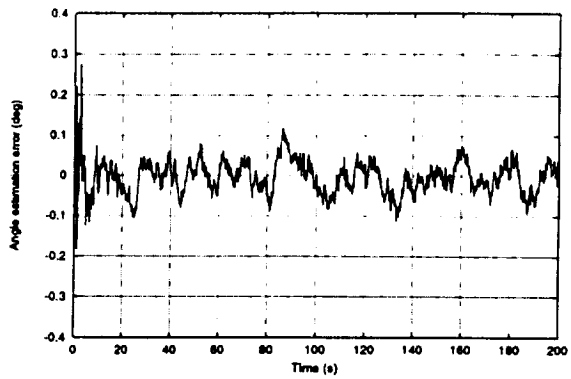

(b) Roll – with vector observation aiding

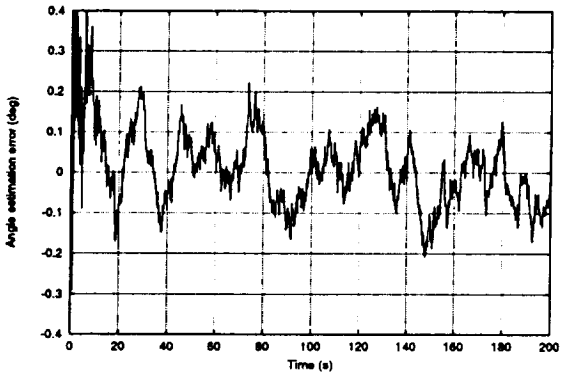

(c) Pitch – GPS only

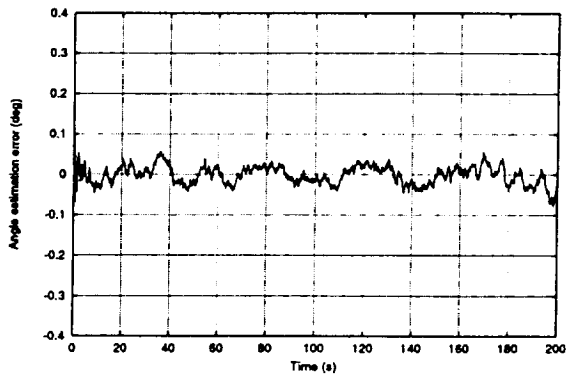

(d) Pitch – with vector observation aiding

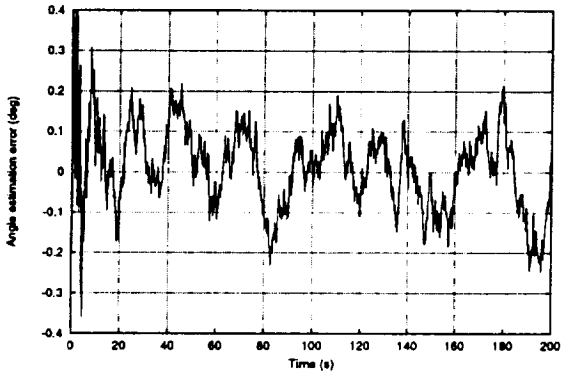

(e) Yaw – GPS only

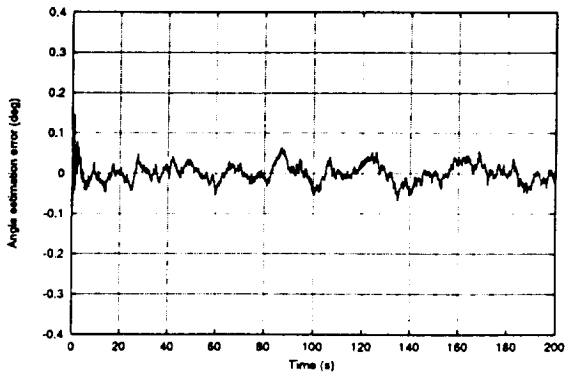

(f) Yaw – with vector observation aiding

Fig. 3: Example I: The effect of vector observation aiding on Euler angle estimation.

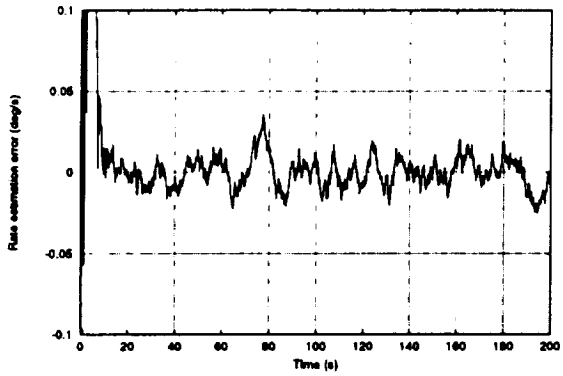

(a) ω_1 – GPS only

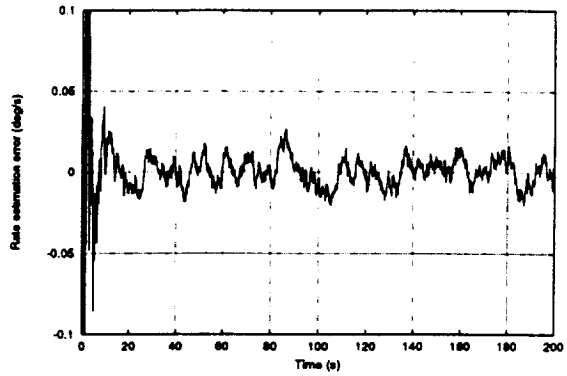

(b) ω_1 – with vector observation aiding

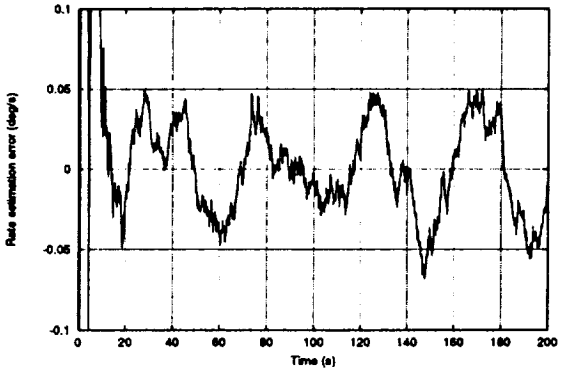

(c) ω_2 – GPS only

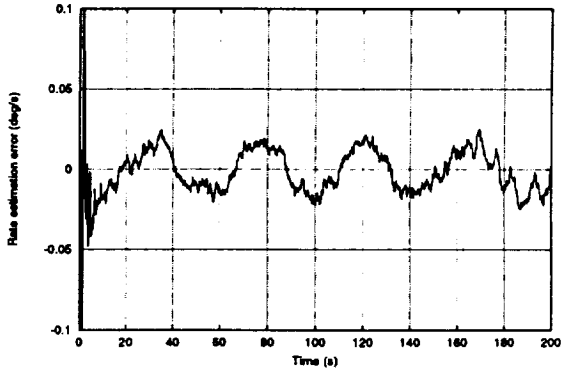

(d) ω_2 – with vector observation aiding

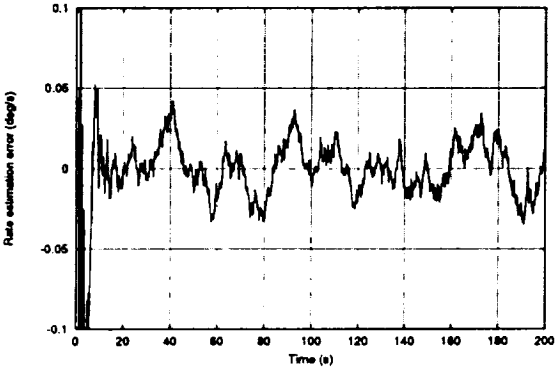

(e) ω_3 – GPS only

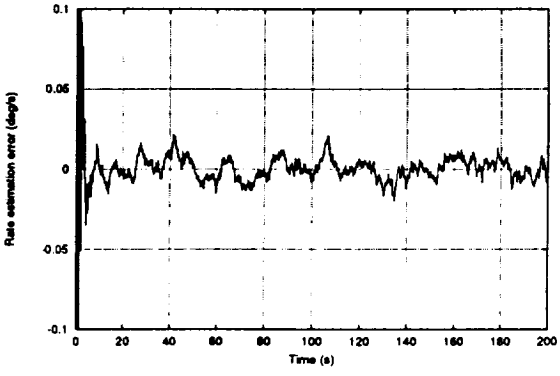

(f) ω_3 – With vector observation aiding

Fig. 4: Example I: The effect of vector observation aiding on angular rate estimation.

Table 1: Example I: The effect of vector observation aiding on estimation performance.

	GPS only		Vector observation aiding	
	Mean	Standard deviation	Mean	Standard deviation
Roll angle (deg)	-9.2×10^{-4}	5.8×10^{-2}	-4.2×10^{-3}	3.9×10^{-2}
Pitch angle (deg)	3.0×10^{-3}	8.1×10^{-2}	-1.4×10^{-3}	2.2×10^{-2}
Yaw angle (deg)	7.1×10^{-3}	9.5×10^{-2}	9.9×10^{-4}	2.2×10^{-2}
ω_1 (deg/s)	-5.8×10^{-4}	9.5×10^{-3}	5.1×10^{-5}	8.2×10^{-3}
ω_2 (deg/s)	2.0×10^{-4}	2.7×10^{-2}	-2.8×10^{-4}	1.2×10^{-2}
ω_3 (deg/s)	4.0×10^{-5}	1.5×10^{-2}	3.9×10^{-4}	6.5×10^{-3}

vector observation aiding in reducing the estimation errors standard deviation.

Example II

In this example, the same parameters were used as in Example I, except for the following. The three baselines used were now $\bar{b}_1 = [0.1, 1.0, 0.1]^T$, $\bar{b}_2 = [0.0, 1.0, 0.0]^T$, $\bar{b}_3 = [0.0, 0.0, 1.0]^T$. As can be observed, the first two baselines are almost colinear. The angular velocity of the satellite was $\omega = [0, 236, 0]^T$ deg/hr, which is typical for an Earth-pointing, low Earth orbit satellite, with pitch rate of one revolution per orbit. The Singer angular acceleration model parameters were set to $\tau = 10$ s, $\dot{\omega}_M = 10^{-5}$ rad/s^2, $p_M = p_0 = .001$ for all three axes. As in the first example, vector measurements, when available, corresponded to a randomly selected vector, which was kept constant throughout the run.

In Fig. 5, the three true Euler angles are shown for a typical run. Fig. 6 shows the Euler angle estimation errors (the estimated angles were computed from the estimated attitude matrix assuming a 3-2-1 Euler angle sequence). Fig. 7 presents the angular rates estimation errors for the same run, with and without vector measurement aiding. The estimation error statistics are presented in Table 2. As can be observed, especially from Fig. 6 and Table 2, the robustifying effect of aiding the GPS measurements with vector observations is very

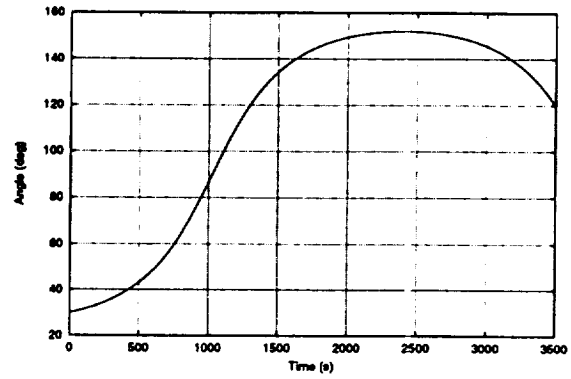

(a) Roll angle

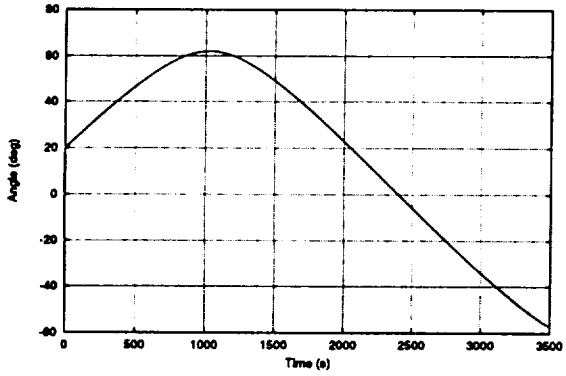

(b) Pitch angle

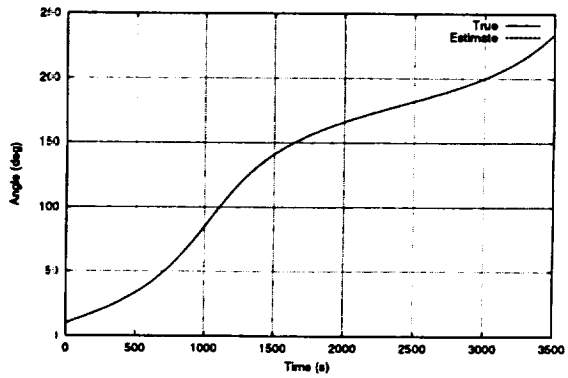

(c) Yaw angle

Fig. 5: Example II: True Euler angles.

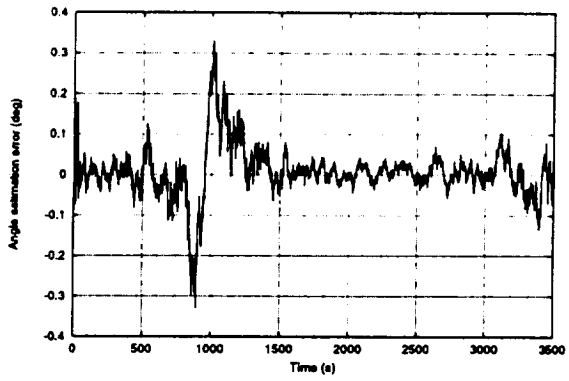

(a) Roll – GPS only

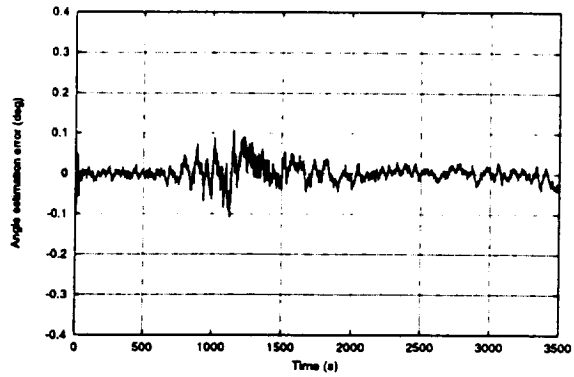

(b) Roll – with vector observation aiding

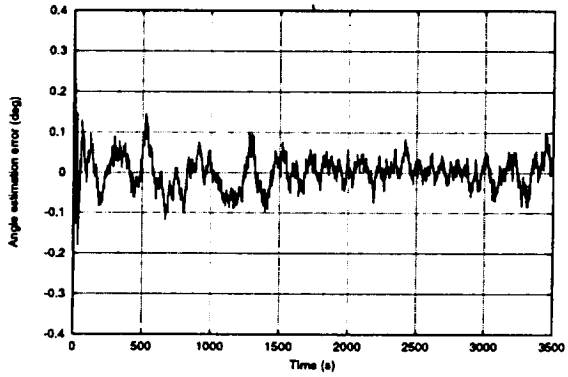

(c) Pitch – GPS only

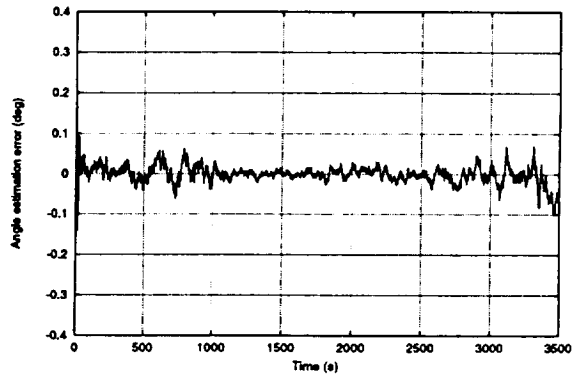

(d) Pitch – with vector observation aiding

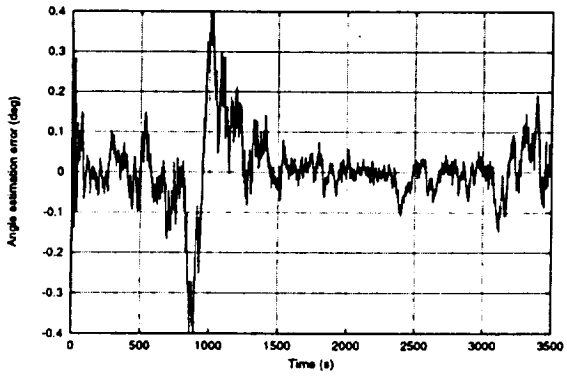

(e) Yaw – GPS only

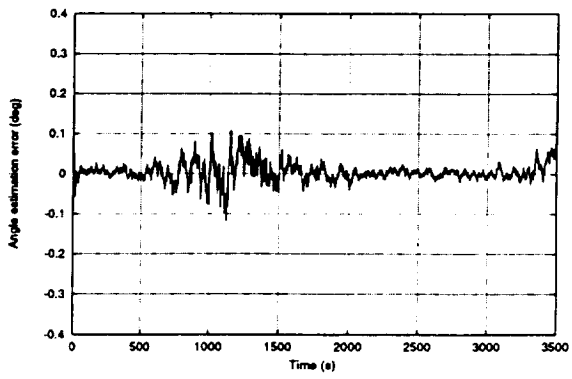

(f) Yaw – with vector observation aiding

Fig. 6: Example II: The effect of vector observation aiding on Euler angle estimation.

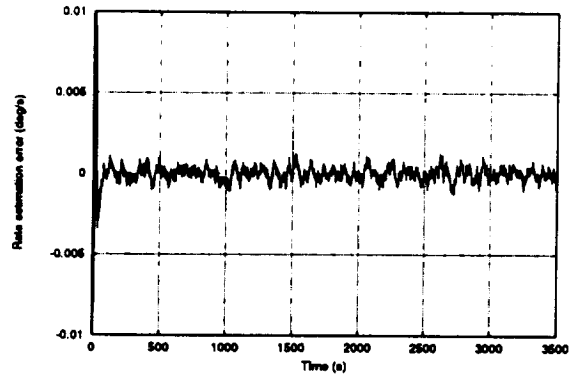

(a) ω_1 – GPS only

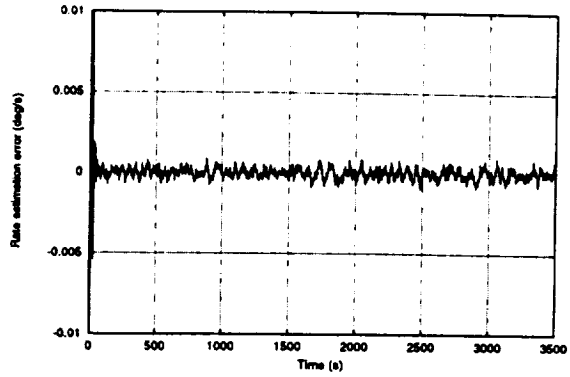

(b) ω_1 – with vector observation aiding

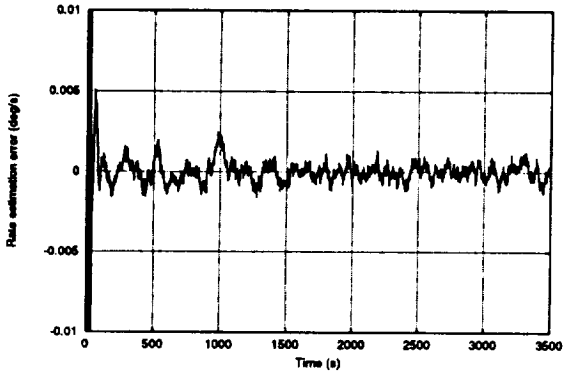

(c) ω_2 – GPS only

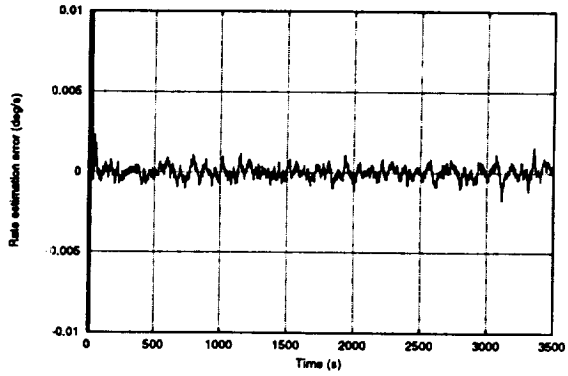

(d) ω_2 – with vector observation aiding

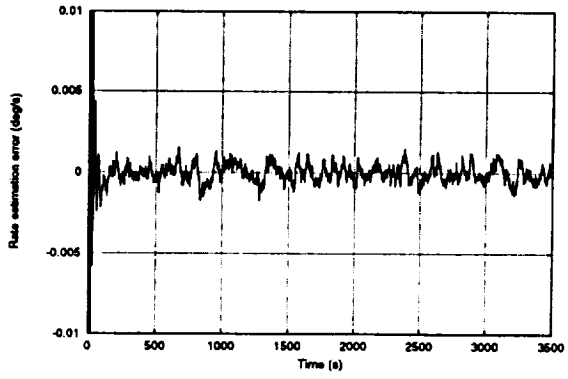

(e) ω_3 – GPS only

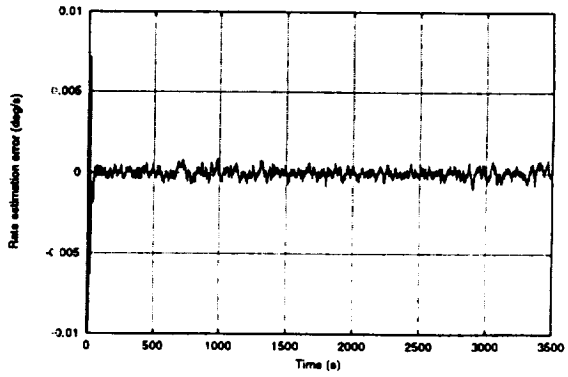

(f) ω_3 – with vector observation aiding

Fig. 7: Example II: The effect of vector observation aiding on angular rate estimation.

Table 2: Example II: The effect of vector observation aiding on estimation performance.

	GPS only		Vector observation aiding	
	Mean	Standard deviation	Mean	Standard deviation
Roll angle (deg)	7.2×10^{-3}	6.4×10^{-2}	1.3×10^{-3}	2.0×10^{-2}
Pitch angle (deg)	1.1×10^{-3}	3.8×10^{-2}	-4.8×10^{-4}	2.0×10^{-2}
Yaw angle (deg)	7.7×10^{-3}	8.7×10^{-2}	4.6×10^{-3}	2.2×10^{-2}
ω_1 (deg/s)	-9.6×10^{-6}	4.8×10^{-4}	2.5×10^{-6}	3.3×10^{-4}
ω_2 (deg/s)	2.8×10^{-5}	9.9×10^{-4}	3.7×10^{-5}	5.1×10^{-4}
ω_3 (deg/s)	3.4×10^{-6}	9.3×10^{-4}	-5.8×10^{-6}	3.5×10^{-4}

significant in this ill-conditioned case.

VIII Conclusions

A nonlinear sequential estimator has been presented, that uses differential GPS carrier phase measurements to estimate both the attitude matrix and the angular velocity of a spacecraft. The algorithm is based on the IRP third-order minimal parametrization of the attitude matrix, which is at the heart of its computational efficiency. Avoiding the use of the typically uncertain (and frequently unknown) spacecraft dynamic model, the filter uses a polynomial state space model, in which the spacecraft angular acceleration is modeled as an exponentially autocorrelated stochastic process. When vector observations are available (e.g., from low accuracy Sun sensors or magnetometers), the estimator's structure can be easily modified to exploit this additional information and, thereby, significantly enhance the algorithm's robustness and accuracy. Numerical examples have been presented, that demonstrate the performance of the proposed algorithm and the advantages of aiding the GPS carrier phase signals with vector observations, even when the vector measurements are of relatively low accuracy.

Acknowledgement

This work was performed while the first author held a National Research Council—NASA Goddard Space Flight Center Research Associateship.

References

[1] Cohen, C. E., "Attitude Determination," *Global Positioning System: Theory and Applications, Vol. II*, edited by B. W. Parkinson and J. J. Spilker, Progress in Astronautics and Aeronautics, AIAA, Washington, D.C., 1996.

[2] Crassidis, J. L. and Markley, F. L., "Attitude Determination Using Global Positioning System Signals," *Proceedings of the AIAA Guidance, Navigation and Control Conference*, New Orleans, LA, Aug. 1997, pp. 23–31.

[3] Bar-Itzhack, I. Y., Montgomery, P. Y., and Garrick, J. C., "Algorithms for Attitude Determination Using GPS," *Proceedings of the AIAA Guidance, Navigation and Control Conference*, New Orleans, LA, Aug. 1997, pp. 841–851.

[4] Fujikawa, S. J. and Zimbelman, D. F., "Spacecraft Attitude Determination by Kalman Filtering of Global Positioning System Signals," *Journal of Guidance, Control, and Dynamics*, Vol. 18, No. 6, Nov.–Dec. 1995, pp. 1365–1371.

[5] Axelrad, P. and Ward, L. M., "Spacecraft Attitude Estimation Using the Global Positioning System: Methodology and Results for RADCAL," *Journal of Guidance, Control, and Dynamics*, Vol. 19, No. 6, Nov.–Dec. 1996, pp. 1201–1209.

[6] Lefferts, E. J. and Markley, F. L., "Dynamic Modeling for Attitude Determination," *Proceedings of the AIAA Guidance and Control Conference*, San Diego, California, Aug. 1976, Paper No. 76-1910.

accuracy.

Acknowledgement

This work was performed while the first author held a National Research Council—NASA Goddard Space Flight Center Research Associateship.

References

[1] C. E. Cohen, "Attitude Determination", in *Global Positioning System: Theory and Applications, Vol. II*, B. W. Parkinson and J. J. Spilker, Eds., Progress in Astronautics and Aeronautics. AIAA, Washington, D.C., 1996.

[2] J. L. Crassidis and F. L. Markley, "Attitude Determination Using Global Positioning System Signals", in *Proceedings of the AIAA Guidance, Navigation and Control Conference*, New Orleans, LA, August 1997, pp. 23–31.

[3] I. Y. Bar-Itzhack, P. Y. Montgomery, and J. C. Garrick, "Algorithms for Attitude Determination Using GPS", in *Proceedings of the AIAA Guidance, Navigation and Control Conference*, New Orleans, LA, August 1997, pp. 841–851.

[4] S. J. Fujikawa and D. F. Zimbelman, "Spacecraft Attitude Determination by Kalman Filtering of Global Positioning System Signals", *Journal of Guidance, Control, and Dynamics*, vol. 18, no. 6, pp. 1365–1371, Nov.–Dec. 1995.

[5] P. Axelrad and L. M. Ward, "Spacecraft Attitude Estimation Using the Global Positioning System: Methodology and Results for RADCAL", *Journal of Guidance, Control, and Dynamics*, vol. 19, no. 6, pp. 1201–1209, Nov.–Dec. 1996.

[16] Bar-Itzhack, I. Y. and Meyer, J., "On the Convergence of Iterative Orthogonalization Processes," *IEEE Transactions on Aerospace and Electronic Systems*, Vol. AES-12, No. 2, Mar. 1976, pp. 146–151.

[17] Oshman, Y. and Markley, F. L., "Minimal-Parameter Attitude Matrix Estimation from Vector Observations," *Proceedings of the AIAA Guidance, Navigation and Control Conference*, New Orleans, LA, Aug. 1997, pp. 12–22, AIAA Paper 97-3451.